Influence of *Elettaria Cardamomum* L. and *Myristica fragrans* Houtt. Seeds on the Thermal Properties and Flammability of Poly(lactic acid)

Tomasz M. Majka

*Email: tomasz.majka@pk.edu.pl

GRAPHICAL ABSTRACT
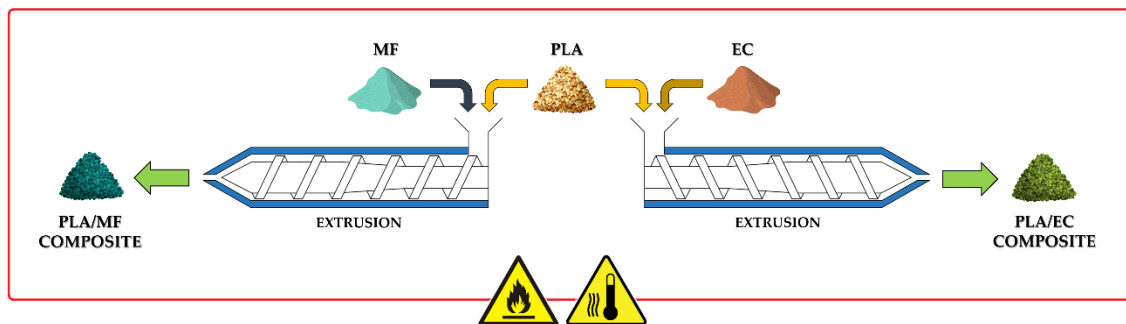
Influence of *Elettaria Cardamomum* L. and *Myristica fragrans* Houtt. Seeds on the Thermal Properties and Flammability of Poly(lactic acid)

Tomasz M. Majka ⓘD

Pharmaceutical studies have reported for many years that plants containing antioxidants have many health-promoting properties, mainly due to organic compounds capable of scavenging free radicals. In this work, the activity of two representative plant families was tested: *Elettaria cardamomum* L. *(*EC) and *Myristica fragrans* Houtt*.* (MF). Results indicate that the antioxidants contained in them decompose into gaseous products at temperatures up to about 640 K. The introduction of EC and MF to the biopolymer matrix resulted in a decrease in the thermal stability of the obtained composites. The resulting char residues acted as a local thermal insulator, which led to reduced flammability of poly(lactic acid) (PLA) composites. As a result, the use of 10 wt% EC and 7.5 wt% MF reduced flammability by 37% and 29%, respectively.

INTRODUCTION

In the search for effective biological flame retardants, the keyword becomes "antioxidants." As a rule, these are plant-derived products consisting of substances that show the ability to inhibit the mechanism of further oxidation of highly reactive organic compounds formed by the decomposition of macromolecules (Grant and Chapple 2009; Nie *et al.* 2018; Renard 2019; Amarowicz and Pegg 2020). Antioxidants can be divided into primary and secondary antioxidants. Primary antioxidants, which are designed to eliminate free radicals, include hindered phenols and polyphenols or aromatic amines (Sun *et al.* 2024). Secondary antioxidants include phosphine esters and sulfur compounds which break down hydrogen peroxides (Hamid *et al.* 2012). There are 5 mechanisms of action of antioxidants (Diplock 1994):

- reducing local oxygen concentration
- removal of initiating radicals
- binding of metal ions from catalysts
- decomposition of peroxides
- interrupting the process of hydrogen stripping by active radicals.

In systems without minerals and metal ions, the mechanism of action is to prevent the proliferation of secondary radicals in chain reactions, such as fat peroxidation, initiated and driven by primary radicals. Compounds contributing so such effects include vitamins C and E and carotenoids.

However, it turns out that there is no need for expensive artificial synthesis of antioxidants in the chemical industry, as nature provides products that can be used successfully as natural flame retardant hybrids. Plant exogenous antioxidants contain four groups of compounds: carotenoids (xanthophylls and carotenes), polyphenols (phenolic acids, flavonoids, anthocyanins, lignans, and stilbenes), tocopherols, and vitamins (vitamin E and C) (Xu *et al.* 2017; Chaidech and Matan 2023).

The most well-known group of antioxidants of natural origin are Natural Phenolic Compounds (NPCs). This group primarily includes lignins and tannins (Sen *et al.* 2015; Xia *et al.* 2018; Meng *et al.* 2024). Liu *et al*. (2025) reported that the use of lignin derivatives in poly(vinyl alcohol) composites reduced the maximum Peak in Heat Release Rate (PHRR) index by 39%, the Total Smoke Production (TSP) by 40%, and the Limiting Oxygen Index (LOI) increased by 69% compared to the reference sample. In turn, Prof. Tian's group used lignin and expandable graphite as a carbon source for the cross-linked structure of polyurethane foam coated with ammonium polyphosphate. Such a hybrid P/C/O system contributed to reducing PHRR by 70% and TSP by 59% (Tian *et al.* 2024). A method for obtaining a flame-retardant material containing purified lignin nanoparticles was also developed. The sequential chemical modification of nitrogen and phosphorus using polyethyleneimine (PEI) and phytic acid (PA) resulted in an increase in the char residue by ≥10 % compared to unmodified lignin nanoparticles (Won et al. 2024). Also, Costes *et al.* (2016) found that P-N chemically treated lignin reduced the thermal degradation of PLA during both melt processing and TGA experiments and significantly improved the flame retardancy properties, enabling it to achieve a V0 classification in the UL-94 test. Finally, Majka (2023b) proposed a two-step method for the synthesis of lignosulfonamides by modifying calcium lignosulfonate to lignosulfonyl chloride and then reacting it with a secondary amine. The lignosulfonamides obtained were subsequently tested for thermal stability and flammability. As a result of proposing four different synthesis routes for lignosulfonyl chloride in the first step and three types of amines used (dibutylamine, N-butyl-N-dodecylamine and didodecylamine) in the second step, only lignosulfonamides obtained using PCl$_5$ (route B) had negligible flammability and better thermal stability. Jiang *et al.* (2024) also indicated that the deposition of keratin and oxidized tannin on PA66 fabric resulted in the reduction of PHRR and TSP of the fabric by 57% and 52%, respectively, while generating nearly 22% of carbon residue at 800 °C**.** Similarly, functionalization of graphene nanoparticles with *Acacia mangium* tannin resulted not only in a 30% increase in the mechanical strength of the eco-friendly phenolic resin but also in a reduction of the PHRR to the level of 6.9 W/g (Li et al. 2023). The use of an easy adsorption technique of condensed tannin extracted from *Dioscorea cirrhosa* tuber carried out under weak acidic conditions was able to impart good and durable flame retardancy to silk fabric. The tannin-modified fabric showed an LOI above 27%. Thermogravimetric analyses suggested that a significant condensed phase mechanism contributed to the improvement of flame retardancy of silk fabric (Yang *et al.* 2018). Majka *et al.* (2024b) also studied the effect of calcium lignosulfonate (CLS) and tannic acid (TA) on the flammability and thermal properties of PLA composites. As a result of these studies, it turned out that both CLS and TA added directly to polyester are able to reduce the flammability of PLA by more than 30%, maintaining a similar burning time as the pure matrix.

An example of a plant that contains a high number of antioxidants is *Elettaria cardamomum* L. (EC, cardamom). EC is available as dried fruit (capsules), powder (dry seeds), or essential oil (Saloko *et al.* 2014). The essential oil is obtained from the distillation

of the seeds and produces by-products called biomass and shells. Cardamom seeds contain about 30 wt% fiber, while cardamom fruit and rhizome contain mainly starch. Fresh cardamom fruit also contains essential oils, pigments, proteins, cellulose, sugars, silica, potassium oxalate, and minerals (Morsy 2015). GC-MS analysis of the extracted essential oil from fresh EC seeds grown in India showed that about 30 different compounds were present (Alam *et al.* 2019). The main constituents were α-terpinyl acetate and 1,8-cineol, as well as compounds present in amounts of less than 10%, including linalool, α-terpineol, and linalyl acetate (Jena *et al.* 2021; Moulai-Hacene *et al.* 2020). Another study even showed the presence of more than 70 different compounds (Singh *et al.* 2008), with the essential oil extraction from fresh EC fruits yielding more than 70% of 1,8-cineole. During thermo-oxidative decomposition at 573 K, the α-terpinyl acetate present in the EC decomposed with the elimination of acetic acid. Further, a reaction takes place to form limonene, in which hydrogen is removed from the isopropyl group. After hydrogen detaches from the neighbouring tertiary carbon atom, terpinolene is formed. It should be noted that hydrogen transfer can occur during the elimination reaction, so substituted cyclohexadiene molecules can also be formed, resulting in the increased formation of γ-terpinene and α-terpinene. Decomposition of linalyl acetate and linalool occurs through the elimination of acetic acid and water, respectively, to form β-myrcene, trans-β- and cis-β-ocimen (Jakab *et al.* 2018). The seeds of cardamom can be also converted by pyrolysis into liquid smoke and solid biochar (Yaman 2004; Xin *et al.* 2021). Liquid smoke produced up to 623 K has antioxidant properties because it is composed of compounds derived from cellulose, hemicellulose, and lignin, such as acetic acid, carbonyl-containing compounds, furans and furfurals, and phenolic compounds (Mansur *et al.* 2023; Montazeri *et al.* 2013).

The second representative of a plant product that is a carrier of antioxidants is *Myristica fragrans* Houtt. (MF, nutmeg). The primary ingredient of MF is muscat balm fat, which consists of myristic acid triglyceride (Członka *et al.* 2020). The second basic component is an essential oil, which includes α-pinene, camphene, p-cymene, limonene, linalool, geraniol, and borneol. The rest of MF consists of starch, carbohydrates, saponins, and lipases (Muchtaridi *et al.* 2010; El-Alfy *et al.* 2019). GC-MS analysis of the MF acetone extract led to the identification of 32 different compounds accounting for more than 99% of the total extract. Sabinene, β-pinene, α-pinene were found to be the main components of MF. Other important compounds identified were terpinen-4-ol, myristicin, limonene, γ-terpinene, isoeugenol, elemycin, p-cymene, terpinolene, and linalool (Gupta *et al.* 2013). The thermal decomposition process of MF essential oil occurs in three steps. The initial degradation starts with the loss of moisture content at around 373 K. The second thermal degradation begins at 440 K and shows a maximum degradation rate at 503 K, which could be due to the volatilization of constituents of the MF oil. Above 523 K, all MF essential oil should be completely decomposed into volatile degradation products (Amina *et al.* 2021). TGA analysis of granulated and powdered nutmeg seeds revealed 3 stages of decomposition: the drying stage, the gasification stage, and the char formation stage. The drying stage (298 to 393 K) is associated with the release of moisture. Phase 2 (393-783 K) sees the greatest weight loss as cellulose and hemicellulose decompose into gaseous products. In the third stage (783-1173 K), lignin, which is responsible for the formation of char, is decomposed (Ashwini *et al.* 2024).

Even though both EC and MF are prized spices with a distinctive, intense aroma, as well as possessing antibacterial, anti-inflammatory, and digestion-enhancing properties, there are more differences between them than similarities. What both spice sources have in common is the content of essential oils, which have proven pharmacological and

aromatic effects. There are also at least 5 active terpenes in both EC and MF: limonene, α-pinene, camphene, geraniol, and sabinene. EC, on the one hand, is a perennial, while MF comes from a tree. EC mainly contains 1,8-cyneol, and α-terpineol, while MF has a high content of myristicin, which can be toxic in large quantities.

So far, the author's search for a natural flame retardant for bio-polyesters includes 3 groups of compounds: pyrolysis-recovered flame retardants (Majka *et al.* 2016, 2019; Majka 2023a,b), mineral-derived flame retardants (Majka *et al.* 2018, 2020; Majka 2024a) and natural fiber-derived flame retardants (Majka *et al.* 2024a). It turned out that of all the additives tested, the most effective were compounds of plant origin, making it possible to achieve up to 30% reduction in PLA flammability (Majka *et al.* 2024b). However, that level of achieved result is still too low to compete with commercial phosphorus flame retardants. Therefore, in this study it was decided to check the effect of powdered seeds of *Elettaria cardamomum* L. and *Myristica fragrans* Houtt. on the flammability of polylactide. These seeds were chosen due to their different composition, especially of polyphenols, terpenes, fats, as well as lignin. It was expected that it was the amount of lignin that would play a special role in the mechanism of reducing the flammability of polylactide at temperatures above 623 K. This is of great importance because the total global production of cardamom is estimated at 55,000 to 60,000 tons per year, while the global production of nutmeg is about 100,000 to 120,000 tons per year ("Nutmeg, mace and cardamons (HS: 0908) Product Trade, Exporters and Importers | The Observatory of Economic Complexity" n.d.).

EXPERIMENTAL

Materials

Poly(lactic acid) (PLA, CAS No. 26100-51-6, M_w = 116000 Da, PDI = 1.83 (Majka et al. 2024b)) dedicated for injection molding, with the trade name Ingeo™ Biopolymer 3052D was purchased from NatureWorks (Blair, USA). *Elettaria cardamomum* L. (EC, CAS No. 8000-66-6) fruit powder was purchased from BOS Natural Flavors (P) Ltd. (Kerala, India). *Myristica fragrans* Houtt. (MF, CAS No. 84082-68-8) seed powder was also provided by BOS Natural Flavors (P) Ltd. (Kerala, India).

Methods

The morphology and structure of the obtained composites and raw materials were examined by Fourier Transform Infrared Spectroscopy (FTIR) and Scanning Electron Microscopy (SEM). A Perkin Elmer Spectrum 65 spectrometer (Perkin Elmer, Krakow, Poland) equipped with an ATR attachment and a diamond/ZnSe crystal was used for the FTIR analysis. The tests were performed within the spectral range of 4000 to 500 cm^{-1} with 16 scans.

A JEOL JSM-6010LA analytical scanning electron microscope (JEOL Ltd., Tokyo, Japan) was used to check the distribution of additive particles in the biopolymer matrix. Microphotographs were taken at an accelerating voltage of 10 kV and a working distance of 10 mm. Before examination, each sample was sputtered with a 4 nm thick layer of gold.

The obtained PLA biocomposites and raw materials were tested for thermo-oxidative degradation (TGA) using a NETZSCH TG 209F1 Libra (Netzsch, Krakow, Poland) apparatus. The test was carried out in an oxidizing atmosphere (air flow 15

cm^3/min) under the following conditions: temperature range from 298 K to 873 K; heating rate 10 K·min^{-1}.

Differential scanning calorimetry (DSC) were carried out using a Mettler Toledo DSC823e (Mettler Toledo, Warsaw, Poland) apparatus. The measurement was carried out in an inert atmosphere according to the following temperature programs:

- heating 298 – 443 K at a rate of 10 K·min^{-1},
- cooling 443 – 298 K at a rate of 10 K·min^{-1},
- heating 298 – 443 K at a rate of 10 K·min^{-1}.

Pyrolysis-combustion flow calorimetry (PCFC) was carried out using a Fire Testing Technology (FTT, East Grinstead, UK) apparatus. Composite tests were conducted in the temperature range of 423 to 1023 K at a heating rate of 1 K·s^{-1}.

Sample Preparation

The purpose of the work was to test the effect of antioxidants contained in unmodified seeds of known spices on the flammability of the polylactide matrix. For this purpose, the powdered EC and MF seeds were pre-dried at 353 K for 48 h (OV-11 vacuum oven, Jeio Tech Co., Chalgrove, UK) to achieve a water content of less than 0.05 %. The preparation process (Fig. 1) used a processing line consisting of a Brabender DR20 feeder (RHL-Service, Poznań, Poland), a Haake Rheomex OS PTW 16/25 twin-screw extruder (RHL-Service, Poznań, Poland), a Zamak W1500 cooling bath (Zamak Mercator, Skawina, Poland), and a Zamak G-16/325 granulator (Zamak Mercator, Skawina, Poland). Processing conditions are shown in Table 1.
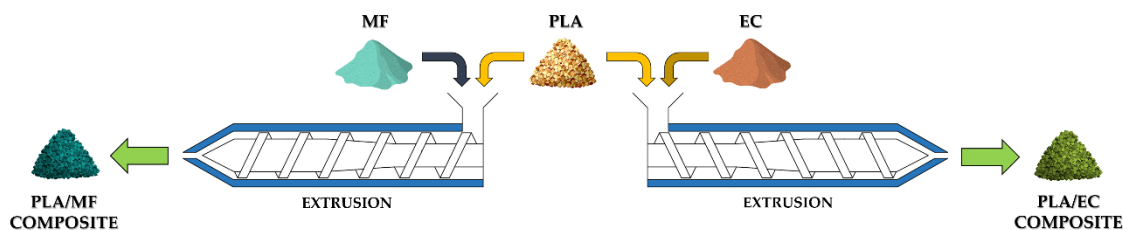
Fig. 1. Diagram showing the pathway for obtaining polylactide composites with EC and MF

Using this co-rotating extruder, PLA/EC, and PLA/MF composites containing a total of 1.0, 2.5, 5.0, 7.5, and 10.0 wt% of filler were obtained.

Table 1. High-Temperature Extrusion Conditions for PLA Composites

Extrusion							
	Heating zones						
	1	2	3	4	5	6	Die
Temperature (K)	473	473	478	478	483	483	483
Degassing	-	-	-	-	Yes	-	-
Screws speed (min⁻¹)	150						
Feed capacity (%)	5						
Cooling bath							
Temperature (K)	293						
Compression press							
Temperature of stamps (K)	483						
Pressure (MPa)	24						
Pressing time (s)	420						

RESULTS AND DISCUSSION

Morphology and Structure of the Obtained Composites

Figure 2 shows the FTIR spectra of the raw materials EC and MF. Although the introduction indicated certain similarities in the structure of both compounds, the superposition of the FTIR spectra allowed for the assessment of their common features. In both cases, the visible peak for the absorption band at 3300 cm^{-1} confirmed the presence of OH groups, for example, in α-terpineol or geraniol.

The FTIR spectrum of EC with bands in the region between 900 and 716 cm^{-1} was associated with the presence of C=C and =CH of aromatic rings and CH out-of-plane vibrations from the α-terpinyl derivatives (Dehghani *et al.* 2020; Karimi *et al.* 2020). In addition, the vibrational interactions of the OH group (1078 cm^{-1}) and the C-C bond (1177 cm^{-1}) were also present in EC, respectively (Cebi *et al.* 2021; Truzzi *et al.* 2021). In turn, elongation interactions of carboxylic acid, carbonyl ester, and carbonyl groups were observed at the absorbance bands of 1250, 1735, 2948, and 2910 cm^{-1} (Ni *et al.* 2020; Salvia-Trujillo *et al.* 2015).

The FTIR spectrum of MF with bands at 1633, 1512, 1470, 1177, 1114, and 997 cm^{-1} confirmed the presence of myristin in its composition (Dupuy *et al.* 2013). Characteristic peaks located at 2910 cm^{-1} (vibration OH group) and 2848 cm^{-1} (vibration -CH_2 group) correspond to the presence of cellulose, hemicellulose, and lignin. The band located at 1735 cm^{-1} corresponds to the carbonyl vibration (C=O) from α-terpinyl. The peak centered at 1633 cm^{-1} indicated the presence of an aromatic ring. The phenol-characteristic bands were found at 1177 to 1114 cm^{-1} (C–OH tensile vibration) (Członka *et al.* 2020).
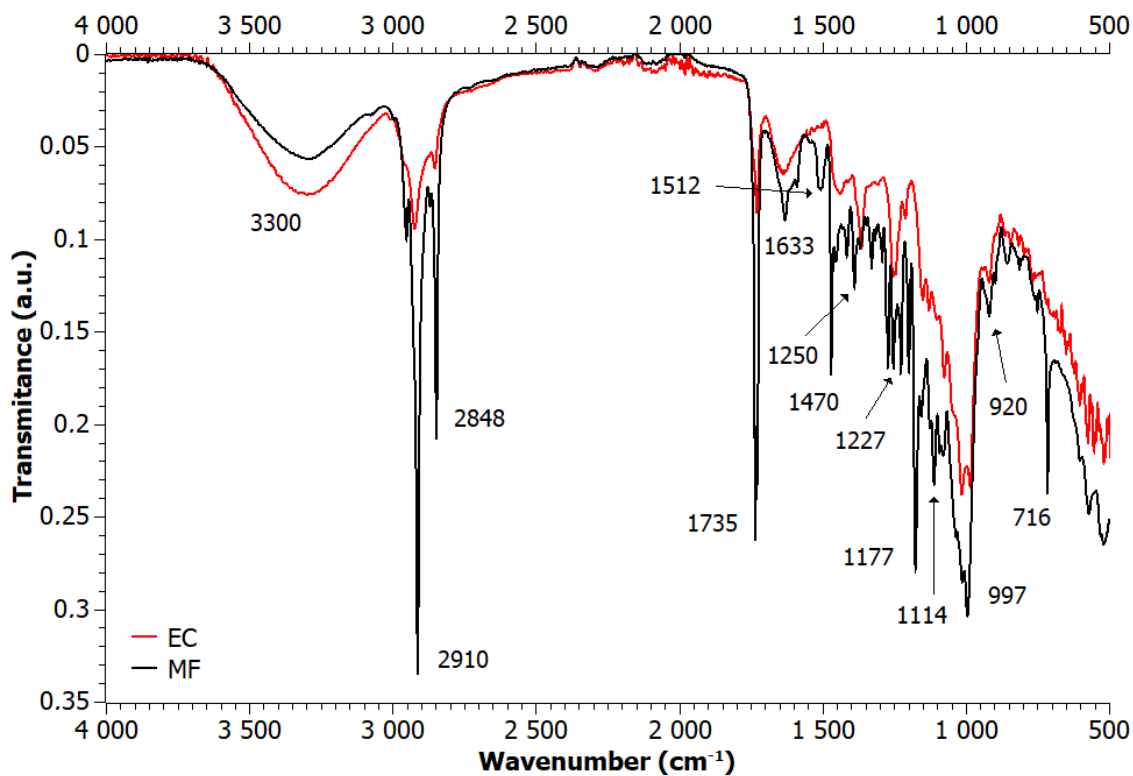
Fig. 2. FTIR spectra of EC and MF raw materials

Selected PLA composites containing 10 wt% biofiller obtained by high-temperature extrusion were also subjected to FTIR analysis (Fig. 3). In both cases, the absorbance bands at wave number 1742 cm^{-1} were due to stretching vibrations of the carbonyl group. In the vicinity of 2938 cm^{-1} range, stretching vibrations corresponding to the CH_3 group were also visible. The peaks at 1448, 1360, and 1179 cm^{-1} were assigned to the -CH- deformation, which included symmetric and asymmetric bending. In the range of wave numbers 1081 to 1040 cm^{-1}, absorbance bands characteristic of C-O and C-C bonds were assigned. Moreover, in the PLA/MF10.0 sample, a broad absorbance band with a maximum of 3345 cm^{-1} was observed, suggesting the presence of OH groups. According to the literature, PLA is characterized by the presence of the following absorbance bands: 1757 cm^{-1} - CO bond stretching, 2996 cm^{-1} and 2945 cm^{-1} bands -CH stretching of -CH_3, 1187 cm^{-1} band - C-O ester stretching (Hoidy *et al.* 2010; Singla *et al.* 2012).
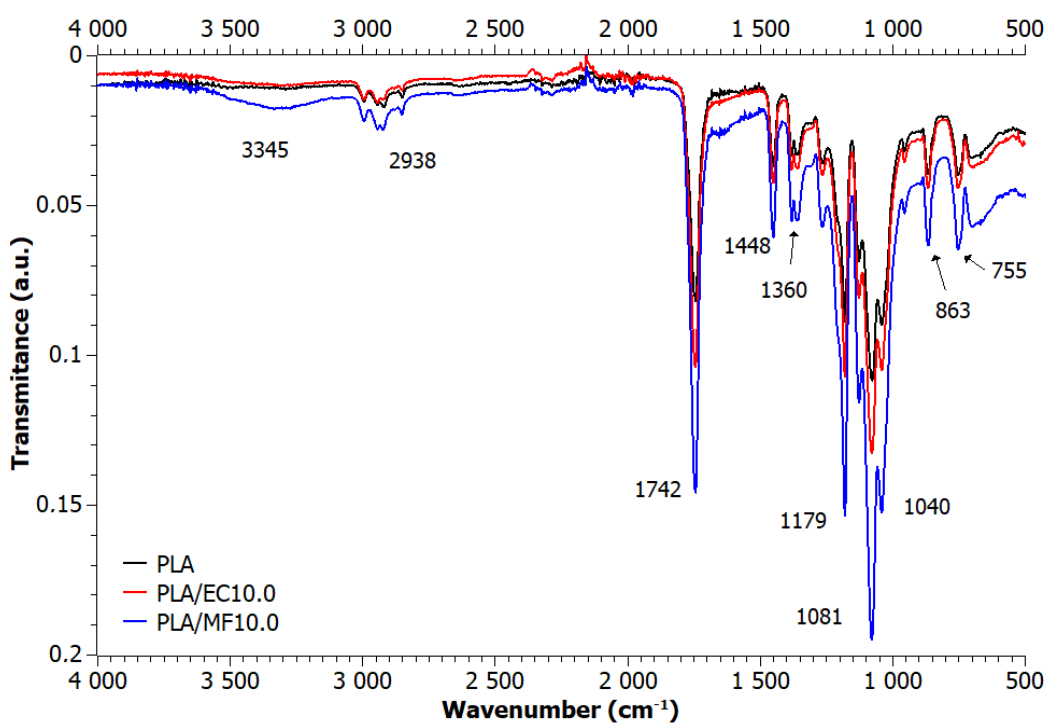

Fig. 3. FTIR spectra of PLA/EC and PLA/MF composites

The remaining overlapping bands could have originated from organic compounds in the fillers. Most of the peaks from PLA overlapped in this wavenumber range with signals from biofillers with a small difference in the range above 3000 cm^{-1}, which made it impossible to distinguish these compounds using the FTIR method. Therefore, to confirm the presence of EC and MF in the composite samples, SEM analysis of the cross-sections of the obtained extrudates was performed. Figure 4 shows SEM micrographs of samples A) PLA/EC10.0 and B) PLA/MF10.0 taken at 1000x magnification.

Analysis of the fracture micrographs of both extrudates revealed a very important difference in the behavior of the biofillers. Namely, the MF particles (Fig. 4B) were completely wetted by the polylactide matrix, while the EC particles remained untouched by it, with a preserved interface. This may mean that MF was a more compatible filler for PLA than EC.
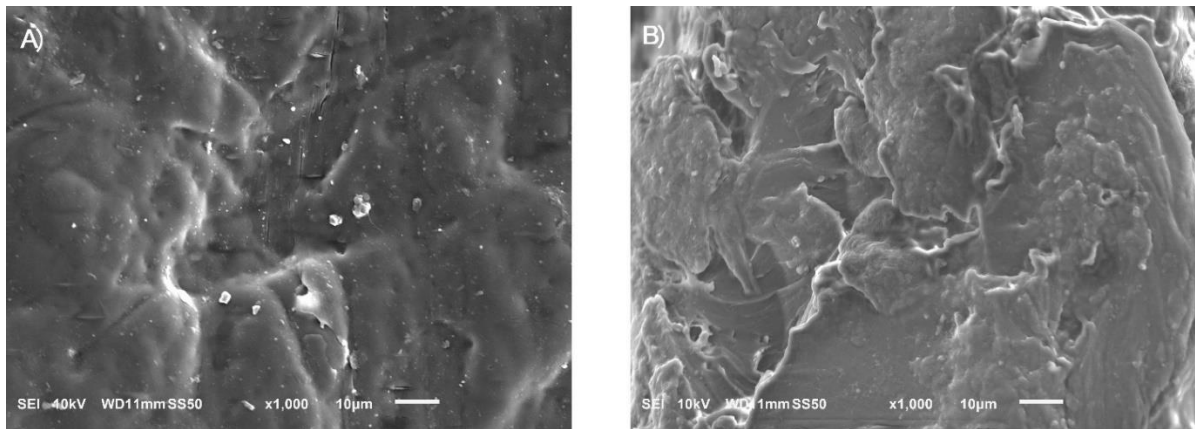
Fig. 4. SEM photos of PLA/EC and PLA/MF composites

In addition, MF was distributed unevenly over the entire surface of the sample, which also suggests a tendency for MF to form agglomerates with a diameter ranging from 3.33 µm to 6.66 µm. In addition, during the analysis of the PLA/MF composite, cracks in the structure were observed. The length of the observed cracks was not uniform; there were smaller cracks around 13 µm and larger ones around 63 µm. The width of the observed cracks ranged from 0.77 to 3.08 µm. From the conducted study, it can be concluded that the stabilization effect using MF occurred only locally, and not, as expected, throughout the entire mass of the sample. In addition, studies at higher magnification confirmed the limited thermal stability of the sample. The observed microcracks on the surface of the composite material during its slight heating could contribute to obtaining worse mechanical properties of samples exposed to elevated temperatures.

SEM analysis of PLA/EC composites revealed a more irregular sample surface than PLA/MF. The presented micrograph (Fig. 4A) indicated the presence of EC agglomerates with sizes close to 10 µm. The presence of EC particles not wetted by the matrix distributed in small areas, which coexisted in the vicinity of micro craters, also affected the surface porosity.

Thermogravimetry analysis (TGA)

Figure 5 shows a plot of the temperature dependence of sample weight change for composites containing EC (A) and MF (B). In addition, to accurately compare the thermal properties of the obtained biomaterials, the corresponding thermogravimetric indices are collected in Table 2. DTG analysis shows that EC decomposed in three stages. The first stage of decomposition was associated with the release of mainly moisture (up to about 410 K). As the temperature increased further, the release of compounds such as 1,8-cineol (about 450 K) and α-terpinyl acetate (about 493 K) occurred, as well as the formation of liquid smoke due to the decomposition of cellulose and hemicellulose. The release of a large amount of volatile degradation products ($T_{5\%}$ mass loss point) only promoted the temporary stabilization of mass loss ($T_{10\%}$-$T_{20\%}$) associated with acetic acid formation. As a result, the resulting acetic acid and its derivatives decomposed rapidly at temperatures above 600 K, resulting in a mass loss of more than 50%. In the last step (640 to 760 K) there was decomposition of lignin reaching nearly 10% residue. In contrast, MF decomposed in four stages, with the first stage of decomposition also associated with the release of moisture and ending just before 400 K. The next phase of decomposition

involved overlapping two mechanisms: the volatilization of essential oil components (404 - 490 K) and the subsequent decomposition of cellulose and hemicellulose into gaseous products (490 to 660 K). The final step also involved the decomposition of lignin (660 to 780 K) to a solid residue of nearly 3%.
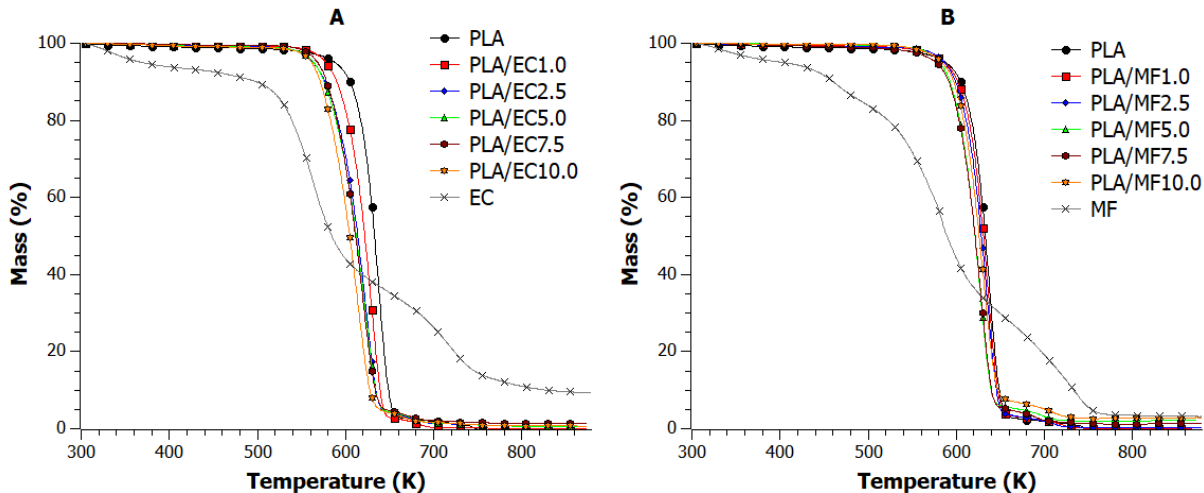

Fig. 5. TGA curves for PLA composites including: A) EC; B) MF

Pure PLA had the highest thermal stability over the entire measurement range of all biomaterials analyzed. PLA decomposed completely to gaseous products, with the first phase of decomposition being the main decomposition stage, in which the biopolymer lost nearly 98% of its mass (up to about 680 K). In contrast, the second step involved the final post-combustion of the residue in the range of 735 to 755 K. Comparing the effects of additives on the thermo-oxidative stability of PLA (Fig. 5), it is worth noting that the degree of filling of the biomatrix with EC played a much greater role than the degree of filling with MF. As the EC content of the PLA/EC composite increased, there was a gradual decrease in thermal stability. While the addition of 2.5, 5.0 and 7.5 wt%. EC practically did not change the thermal characteristics of the composite. What changed was mainly the mass of the residue at 873 K, which was related to the different degrees of homogeneity of EC in PLA. This bio-filler showed a strong tendency to clump during high-temperature processing (especially at higher additive concentrations), which was a major drawback that later disrupted the thermo-oxidative degradation mechanism. Therefore, for the three composites PLA/EC2.5, PLA/EC5.0, and PLA/EC7.5, a very similar result was obtained.

Analysis of the TGA curves of the PLA/MF composites revealed that all the composite samples had even more similar thermal properties. The TGA curves of PLA/MF composites practically overlapped regardless of the amount of powder additive used. Again, there was a problem with the cohesive bonding of MF particles into larger fragments, which increased as the proportion of the additive in the biomatrix increased. As a result, different levels of residues after decomposition at 873 K were also obtained in PLA/MF composites.

Table 2. Summarized TGA Indices Determined for PLA/EC and PLA/MF Composites and Powder Additives

Sample	$T_{5\%}$ (K)	$T_{10\%}$ (K)	$T_{20\%}$ (K)	$T_{50\%}$ (K)	T_{MAX} (K)	Residue at 873 K (%)
EC	369	499	539	584	561	9.34
MF	404	460	523	589	584	3.17
PLA	588	605	617	633	637	0.00
PLA/EC1.0	578	590	603	622	629	0.01
PLA/EC2.5	563	577	591	614	624	0.67
PLA/EC5.0	563	576	589	612	623	0.50
PLA/EC7.5	568	578	590	611	620	1.45
PLA/EC10.0	561	571	583	604	614	0.68
PLA/MF1.0	586	601	614	631	635	0.00
PLA/MF2.5	586	599	611	628	635	0.33
PLA/MF5.0	587	598	610	627	633	2.07
PLA/MF7.5	577	591	603	621	627	1.28
PLA/MF10.0	584	597	608	626	630	2.89

　　　　The agglomeration of EC and MF in the plasticizing system favored obtaining non-homogeneous biocomposites. A local increase in the proportion of EC and MF in the continuous phase caused more char to form. It is worth noting that both PLA/EC and PLA/MF composites decomposed in two stages. For all PLA/EC samples, the main decomposition stage ended at 650 K ± 2 K (97 wt% loss), and the second decomposition stage was in the range of 650 to 705 K and 650 to 700 K for samples containing 1.0, 2.5, 5.0 wt% EC and 7.5 and 10.0 wt% EC, respectively. A slightly different behavior was observed for PLA/MF samples. As the MF content in PLA increased, the T_{EndSet} of the main decomposition step shifted towards lower temperature values (by 5 K for each mass share). This means that the degradation rate of PLA/MF composites depended on the MF content in PLA. Deeper analysis showed that the MF share also affected the shift of the second stage of decomposition toward lower temperatures. The higher the MF share, the greater the shift of the second stage of decomposition.

　　　　The inhomogeneous distribution of the bio-filler in the biomatrix caused more volatile compounds to volatilize in some parts of the composite due to the temperature increase than in other parts, causing the local formation of bubbles encapsulated in the polymer melt. The volatilized decomposition products of cellulose, hemicellulose, essential oils, and their derivatives contributed to the acceleration of the weakening of bonds in the biopolymer chain, consequently leading to their faster breakage. As has been demonstrated, as the amount of bio-filler increased, char formation took place at lower and lower temperatures. Consequently, more char was generated by composites containing MF than EC.

Differential Scanning Calorimetry (DSC)
　　　　Figure 6 shows the DSC curves: (A) for PLA/EC composites and (B) for PLA/MF composites. Detailed analysis of the DSC results made it possible to list the corresponding

indices, which are collected in Table 3, where the degree of crystallinity was calculated using Eq. 1 (Majka 2024b),

$$X_C = \frac{\Delta H_m - \Delta H_{CC}}{(1-\omega) \cdot \Delta H^0} \qquad (1)$$

where ΔH_m is the melting enthalpy of the PLA, ΔH_{CC} is the enthalpy of cold crystallization, and ΔH^0 is the melting enthalpy of a completely crystalline PLA, which is equal to 93 J/g (Majka et al. 2019). The parameter ω is the filler content

During the analysis of the composite systems in the temperature range (300 to 450 K), the following phase transformations were recorded: glass transition, cold crystallization, and melting. Referring to the reference sample (PLA), it was found that regardless of the type of bio-filler introduced and its amount, the glass transition temperature of the composites did not change (± 2 K). This means that both EC and MF did not affect the rate of this transformation.

Despite this, calculated according to Eq. 1, the total degree of crystallinity of polylactide composites depended on the amount of filling introduced. As the EC content increased, the X_c value gradually increased, reaching 0.78 for a 10 wt% fill. The introduction of 1 to 5 wt% MF virtually did not affect the X_c value of PLA/MF composites (0.85). The so-called collapse was observed only at a filling of 7.5 wt%. MF. The presence of bio-fillers in a biopolymer can have two effects: on the one hand, it affects the content of the crystalline phase to in the mass of the biopolymer, and on the other hand, it regulates the formation of the crystalline phase (Majka *et al.* 2024b). In the case considered, the maximum X_c values read for PLA/EC and PLA/MF composites were still lower than for pure PLA. This suggests that both MF and EC acted as a plasticizer, hindering the formation of the crystalline phase. It was noted that only the PLA/MF10.0 sample showed a lower ΔC_p value. These observations suggest that only the addition of 10 wt% MF facilitated the transition from the glassy state to the plastic state, since much less heat needed to be supplied to the system to reach the transition point between the two states.

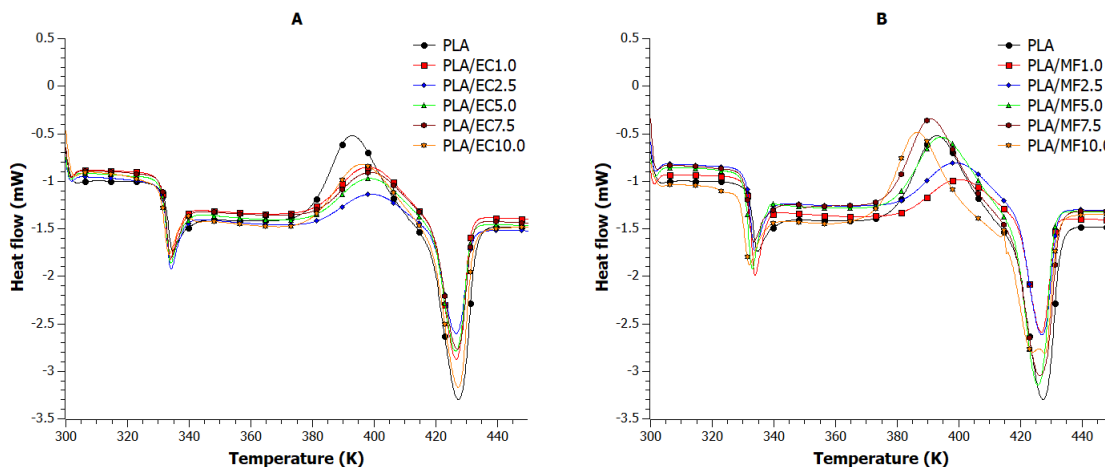**Fig. 6.** DSC curves for PLA composites including: A) EC; B) MF

In all cases, there was a cold crystallization effect, which the author described in more detail in the following references (Majka *et al.* 2016; Majka 2023). Also, all samples showed a shifted T_{cc} point toward higher temperatures, except PLA/MF10.0. In general, EC had virtually no effect on the temperature of the cold crystallization peak, while as the

MF content increased in the range of 5 to 10 wt. %, the T_{CC} peak shifted toward lower temperatures.

All samples, except PLA/MF10.0, were characterized by a single melting peak. This means that a high MF content led to the formation of two PLA phases: a dominant α phase (427 K) and an α' phase (424 K) with a lower proportion. On the other hand, significant changes were observed in the enthalpy of melting values. Low values of H_m for PLA/EC composites mean that the samples melted more easily than pure PLA. Conversely, in order to melt PLA/MF5.0, PLA/MF7.5, and PLA/MF10.0 composites, more energy had to be supplied than was required to melt the reference sample. Referring to the TGA results, it should be pointed out that at the T_m (428 K) point where the composites were in the molten state, only 1% weight loss was achieved.

Table 3. DSC Indicators for PLA/EC and PLA/MF Composites

Sample	T_g (K)	ΔC_p (J/gK)	T_{cc} (K)	ΔH_{cc} (J/g)	T_{m1} (K)	T_{m2} (K)	ΔH_m (J/g)	X_c
PLA	332	0.51	391	16.59	---	428	17.48	0.96
PLA/EC1.0	332	0.49	398	15.57	---	427	15.75	0.22
PLA/EC2.5	332	0.47	400	8.20	---	427	8.55	0.39
PLA/EC5.0	332	0.48	400	9.73	---	427	10.17	0.50
PLA/EC7.5	332	0.48	400	10.57	---	427	11.17	0.70
PLA/EC10.0	332	0.47	396	11.83	---	427	12.55	0.78
PLA/MF1.0	331	0.47	400	10.13	---	427	10.92	0.86
PLA/MF2.5	331	0.46	399	12.68	---	427	13.45	0.85
PLA/MF5.0	330	0.47	394	21.69	---	426	22.42	0.85
PLA/MF7.5	330	0.45	393	20.92	---	428	21.10	0.20
PLA/MF10.0	330	0.33	387	19.21	424	428	19.33	0.14

Labels: melting temperature (T_m), melting enthalpy (ΔH_m), degree of crystallinity (X_c), heat capacity (ΔC_p), cold crystallization temperature (T_{cc}), enthalpy of cold crystallization (ΔH_{CC}) and glass transition temperature (T_g)

Pyrolysis-combustion Flow Calorimetry (PCFC)

The results of the flammability tests are shown in Fig. 7. The analysis of the Heat Released Rate (HRR) *vs.* Temperature curves was reinforced by comparing the flammability indices summarized in Table 4.

Pure EC burned in three stages, reaching a peak heat release rate (PHRR) of 99 W/g (574 K). MF burned over a minute longer than EC, reaching a peak point of 98 W/g (631 K). These bio-fillers, although they burned for a long time, showed low (for these organic materials) heat of combustion (HOC) and total heat release rate (THR). Therefore, their presence in the composite system was expected to contribute to the inhibition of the biopolymer combustion process, especially at high matrix filling. As shown by the data collected in Table 4, these predictions proved to be correct, as at PLA filling of 10 wt% EC and 7.5% wt. MF, a 37% and 29% reduction in flammability was achieved, respectively. The reference sample burned very quickly to gaseous products, in just 127 s, while reaching a peak PHRR of 584 W/g (654 K). Importantly, the PLA/EC10.0 composite burned in a slightly longer time (155 s) achieving the best result of all tested materials.
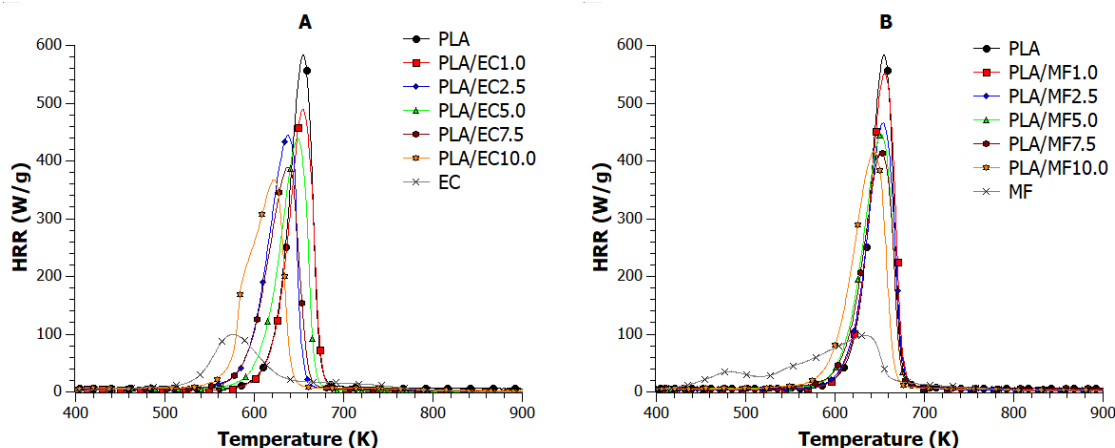
Fig. 7. Heat Released Rate vs Temperature curves for PLA composites with A) EC and B) MF

Table 4. List of Flammability Indicators for EC, MF and PLA Composites

Sample	PHRR (W/g)	HRR$_{AV}$ (W/g)	HOC$_{AV}$ (kJ/g)	THR$_{600s}$ (kJ/g)	TTI (s)	TTI (K)	TOF (s)	TOF (K)	Combustion time (s)
EC	99	13.36	5.62	9.46	87	411	523	842	436
MF	98	19.35	7.86	13.21	38	389	542	851	504
PLA	584	33.94	11.64	22.38	267	577	394	707	127
PLA/EC1.0	490	26.61	9.52	18.20	252	551	442	747	190
PLA/EC2.5	445	28.37	10.77	19.43	220	529	392	706	172
PLA/EC5.0	440	26.94	10.17	18.52	230	545	421	741	191
PLA/EC7.5	389	26.85	10.35	18.82	213	515	407	714	194
PLA/EC10.0	368	28.18	11.09	19.32	206	513	361	673	155
PLA/MF1.0	551	31.61	11.00	21.52	266	560	417	717	151
PLA/MF2.5	465	30.20	10.67	20.06	233	553	411	737	178
PLA/MF5.0	446	30.17	10.83	20.72	220	519	448	754	228
PLA/MF7.5	416	30.72	10.90	20.23	174	501	405	737	231
PLA/MF10.0	416	29.91	11.17	20.84	209	508	435	740	226

Notes: PHRR – peak of heat released rate; HRR$_{AV}$ – average heat released rate; HOC$_{AV}$ – average heat of combustion; THR$_{600s}$ – total heat released after 600 s; TTI – time to ignition; TOF – time out flame

The author is researching green flame retardants of natural origin dedicated to biopolymers, including polylactide. Table 5 summarizes the best results achieved in the author's previous work, where PLA/EC and PLA/MF composites were also included in the ranking. The percentage of reduction in the PHRR index of the tested material relative to PLA was assumed as flammability reduction. According to the literature (Schartel *et al.* 2016a,b), the maximum value of the HRR *vs.* Temperature or HRR *vs.* Time curve can be considered as the comparable flammability level of a given material relative to a reference sample. It turned out that using 10 wt%. EC made it possible to achieve the best result

among all the indicated research works. In contrast, the use of 7.5 wt% and 10.0 wt%. MF reached ex aequo placed 5 in this ranking.

Table 5. Ranking List of Additives Used in the Author's Previous Works that Resulted in the Best Reduction of PLA Flammability

Type of composite	Type of additive	Ammount of additive	Flammability reduction (%)	Reference
PLA/EC	*Elettaria Cardamomum L.*	10 wt. %	37	This study
PLA/CLS	Calcium lignosulfonate	9 wt. %	33	(Majka *et al.* 2024b)
PLA/TA	Tannic acid	9 wt. %	30	(Majka *et al.* 2024b)
PLA/BMT	Tannic acid adsorbed on calcium lignosulfonate	6 wt. %	30	(Majka *et al.* 2024b)
PLA/MF	*Myristica fragrans Houtt.*	7.5 wt. %	29	This study
PLA/SF-BMIC	Pyrolyzed montmorillonite purified with 1-butyl-3-methylimidazolium chloride	5 wt. %	23	(Majka 2024b)
PLA/SF-BMAC	Pyrolyzed montmorillonite purified with methyldodecylbenzyl trimethyl ammonium chloride	5 wt. %	23	(Majka 2024b)
15BL(PLA/NS)	Composite coated with bilayers consists of chitosan and nanosilica	15 bilayers	22	(Majka 2024a)
PLA/UD	*Urtica dioica* fibers	15 wt. %	20	(Majka *et al.* 2024a)
PLA/MUD	*Urtica dioica* fibers treated with a 10% NaOH solution	10 wt. %	20	(Majka *et al.* 2024a)
PLA/MVV	*Vitis vinifera* fibers treated with a 10% NaOH solution	5 wt. %	20	(Majka *et al.* 2024a)
PLA/VV	*Vitis vinifera* fibers	5 wt. %	19	(Majka *et al.* 2024a)
PLA/NS	Nanosilica	5 wt. %	16	(Majka 2024a)
PLA/MMT	Montmorillonite	5 wt. %	5	(Majka 2024b)

Figure 8 shows the temperature dependence of the decomposition reaction rates of PLA/EC (A and C) and PLA/MF (B and D) composites, for the TGA (A and B) and PCFC (C and D) methods, respectively. From the data presented, it can be seen that with slow heating (TGA) of both PLA/EC and PLA/MF composites, the peak of the decomposition reaction rate (RR) curves always occurred at lower temperatures than in the case of rapid temperature rise (PCFC). As the amount of filler in the samples increased, the difference in the shift between the two peaks of the RR curves determined for the same composite gradually decreased, from 25 K for 1.0 wt% content to 7-8 K for 10.0 wt% content.
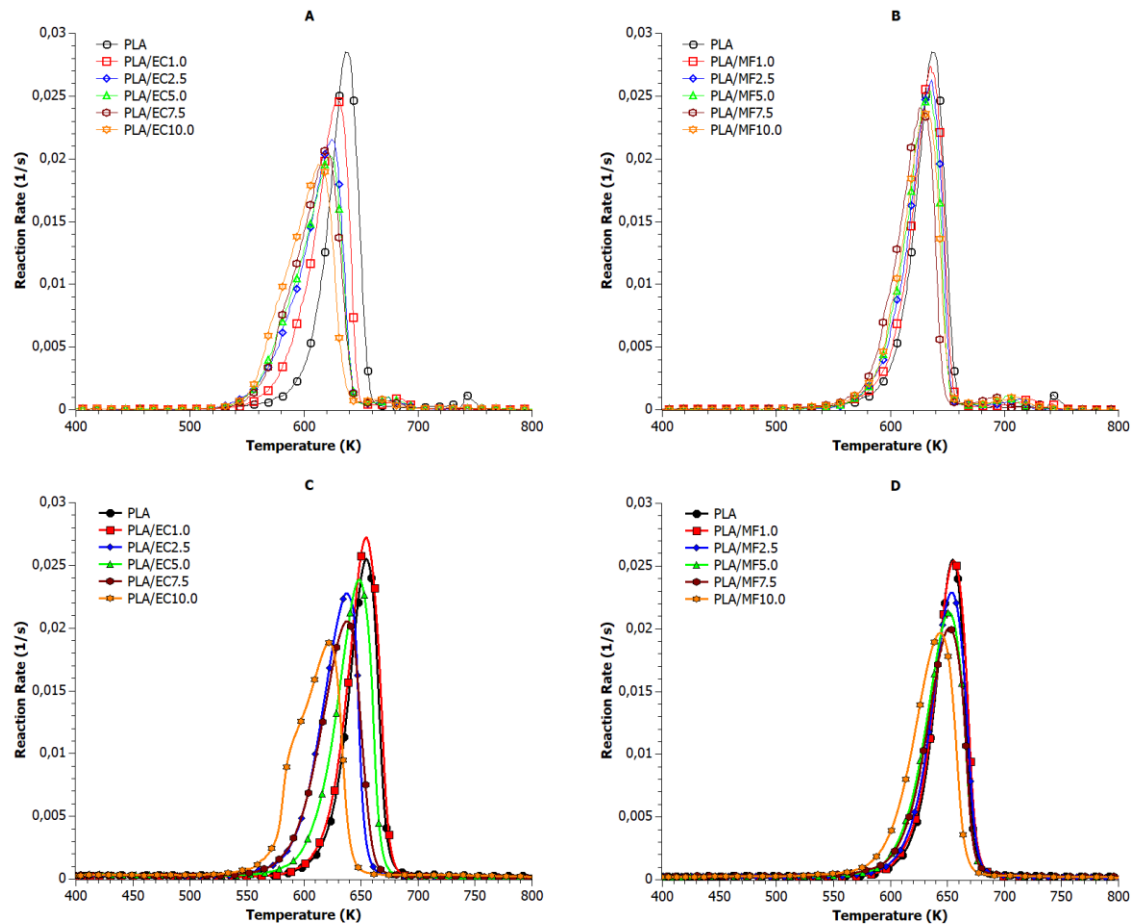
Fig. 8. Temperature dependence of the decomposition reaction rates of PLA/EC (A and C) and PLA/MF (B and D) composites, for the TGA (A and B) and PCFC (C and D) methods.

The reason for this is that high PLA fill using both EC and MF resulted in low thermogravimetric indices. These composites were more susceptible to decomposition, so the charring process started earlier. The char residues that formed acted as a local thermal insulator, resulting in the achievement of reduced flammability. In addition, rapid heating of the biocomposites (1 K/s), as well as increasing the proportion of fill in the sample, influenced the acceleration of decomposition processes leading ultimately to the char formation.

The flame retardancy mechanism is related to the transfer of free radicals on carbon planes (Hou *et al.* 2024). The formed amorphous carbon (a-C) planes can also act synergistically with other compounds, such as phosphorus compounds, to form effective flame retardant coatings (Ma and Fang 2012). In a-C, carbon atoms occur in an ordered manner in a short range, and the chemical bonds between atoms are a mixture of sp^2 and sp^3 hybrid bonds. Therefore, the properties of amorphous carbon are variable depending on its formation conditions (Kouchi 2011).

CONCLUSIONS

1. Both *Elettaria cardamomum* L. (EC) and *Myristica fragrans* Houtt. (MF) decompose into gaseous products and a char residue. Decomposition into gaseous products led to

a mass loss of more than 50%. The formation of a char residue in both cases was due to the decomposition of lignin in the range of 640 to 780 K.

2. High poly(lactic acid) (PLA) filling using both EC and MF increased the susceptibility of the composites to thermo-oxidative decomposition. However, PLA/EC composites were less thermally stable than PLA/MF composites.

3. The formation of solid residue in composites containing EC started much earlier than in PLA/MF composites. The char residues that were formed acted as a local thermal insulator, which resulted in the achievement of reduced flammability. As a result, the use of 10 wt% EC filling in PLA reduced flammability by 37%.

4. The obtained result was the best among all previously tested natural systems by the author for use as flame retardants. It shows how huge the potential is hidden in antioxidants. It opens new paths of searching for effective green flame retardants for biopolymers.

REFERENCES CITED

Alam, A., Majumdar, R. S., and Alam, P. (2019). "Systematics evaluations of morphological traits, chemical composition, and antimicrobial properties of selected varieties of *Elettaria cardamomum* (L.) Maton," *Natural Product Communications* 14(12). DOI: 10.1177/1934578X19892688

Amarowicz, R., and Pegg, R. B. (2020). "Protection of natural antioxidants against low-density lipoprotein oxidation," *Advances in Food and Nutrition Research* 93, 251–291. DOI: 10.1016/BS.AFNR.2020.04.002

Amina, M., Al Musayeib, N. M., Alarfaj, N. A., El-Tohamy, M. F., Al-Hamoud, G. A., Al-Yousef, H. M. (2021). Immunomodulatory and antioxidant potential of biogenic functionalized polymeric nutmeg oil/polyurethane/ZnO bionanocomposite," *Pharmaceutics 2021,* 13(12), 2197. DOI: 10.3390/PHARMACEUTICS13122197

Ashwini, K., Resmi, R., and Reghu, R. (2024). "Pyrolysis characteristics and kinetic analysis of coconut shell and nutmeg shell for potential source of bioenergy," *Engineering Science and Technology, an International Journal* 50, 101615. DOI: 10.1016/J.JESTCH.2024.101615

Cebi, N., Arici, M., and Sagdic, O. (2021). "The famous Turkish rose essential oil: Characterization and authenticity monitoring by FTIR, Raman and GC–MS techniques combined with chemometrics," *Food Chemistry* 354, 129495. DOI: 10.1016/J.FOODCHEM.2021.129495

Chaidech, P., and Matan, N. (2023). "Relatively low concentration of cardamon oil vapour for controlling enzymatic browning and maintaining the quality of rambutans," *LWT* 182, 114832. DOI: 10.1016/J.LWT.2023.114832

Członka, S., Strąkowska, A., Kairytė, A., and Kremensas, A. (2020). "Nutmeg filler as a natural compound for the production of polyurethane composite foams with antibacterial and anti-aging properties," *Polymer Testing* 86, 106479. DOI: 10.1016/J.POLYMERTESTING.2020.106479

Dehghani, S., Noshad, M., Rastegarzadeh, S., Hojjati, M., and Fazlara, A. (2020). "Electrospun chia seed mucilage/PVA encapsulated with green cardamonmum essential oils: Antioxidant and antibacterial property," *International Journal of Biological Macromolecules* 161, 1–9. DOI: 10.1016/J.IJBIOMAC.2020.06.023

Diplock, A. T. (1994). "Antioxidants and free radical scavengers," *New Comprehensive Biochemistry* 28(C), 113–130. DOI: 10.1016/S0167-7306(08)60440-8

Dupuy, N., Molinet, J., Mehl, F., Nanlohy, F., Le Dréau, Y., and Kister, J. (2013). "Chemometric analysis of mid infrared and gas chromatography data of Indonesian nutmeg essential oils," *Industrial Crops and Products* 43(1), 596–601. DOI: 10.1016/J.INDCROP.2012.07.073

El-Alfy, A. T., Abourashed, E. A., Patel, C., Mazhari, N., An, H. R., and Jeon, A. (2019). "Phenolic compounds from nutmeg (*Myristica fragrans* Houtt.) inhibit the endocannabinoid-modulating enzyme fatty acid amide hydrolase," *Journal of Pharmacy and Pharmacology* 71(12), 1879–1889. DOI: 10.1111/JPHP.13174

Grant, M. M., and Chapple, I. L. C. (2009). "Antioxidants and periodontal disease," *Food Constituents and Oral Health: Current Status and Future Prospects* 225–239. DOI: 10.1533/9781845696290.2.225

Gupta, A. D., Bansal, V. K., Babu, V., and Maithil, N. (2013). "Chemistry, antioxidant and antimicrobial potential of nutmeg (*Myristica fragrans* Houtt)," *Journal of Genetic Engineering and Biotechnology* 11(1), 25–31. DOI: 10.1016/J.JGEB.2012.12.001

Hamid, M. R. Y., Ab Ghani, M. H., and Ahmad, S. (2012). "Effect of antioxidants and fire retardants as mineral fillers on the physical and mechanical properties of high loading hybrid biocomposites reinforced with rice husks and sawdust," *Industrial Crops and Products* 40(1), 96–102. DOI: 10.1016/J.INDCROP.2012.02.019

Hoidy, W. H., Ahmad, M. B., Al-Mulla, E. A. J., and Ibrahim, N. A. B. (2010). "Preparation and characterization of polylactic acid/polycaprolactone clay nanocomposites," *Journal of Applied Sciences*, 10(2), 97–106. DOI: 10.3923/JAS.2010.97.106

Hou, B., Shan, X., Yin, H., Shen, J., Wang, Q., Fang, J., and Li, J. (2024). "Preparation of green biodegradable lactic acid-based flame-retardant plasticizer for simultaneously enhancing flexibility, flame retardancy, and smoke-suppression of poly(lactic acid)," *Chemical Engineering Journal* 491, 152186. DOI: 10.1016/J.CEJ.2024.152186

Jakab, E., Blazsó, M., Barta-Rajnai, E., Babinszki, B., Sebestyén, Z., Czégény, Z., Nicol, J., Clayton, P., McAdam, K., and Liu, C. (2018). "Thermo-oxidative decomposition of lime, bergamot and cardamom essential oils," *Journal of Analytical and Applied Pyrolysis* 134, 552–561. DOI: 10.1016/J.JAAP.2018.08.003

Jena, S., Ray, A., Sahoo, A., Champati, B. B., Padhiari, B. M., Dash, B., Nayak, S., and Panda, P. C. (2021). "Chemical Composition and Antioxidant Activities of Essential oil from Leaf and Stem of Elettaria cardamomum from Eastern India," *Journal of Essential Oil Bearing Plants* 24(3), 538–546. DOI: 10.1080/0972060X.2021.1937335

Jiang, L., Zhao, J., Zuo, C., Tan, W., Ren, Y., and Liu, X. (2024). "Protein-tannin interactions towards fabricating flame-retardant, UV-resistance, antibacterial and mechanical-reinforced PA66 fabric," *Progress in Organic Coatings* 197, 108798. DOI: 10.1016/J.PORGCOAT.2024.108798

Karimi, N., Jabbari, V., Nazemi, A., Ganbarov, K., Karimi, N., Tanomand, A., Karimi, S., Abbasi, A., Yousefi, B., Khodadadi, E., and Kafil, H. S. (2020). "Thymol, cardamom and Lactobacillus plantarum nanoparticles as a functional candy with high protection against Streptococcus mutans and tooth decay," *Microbial Pathogenesis* 148, 104481. DOI: 10.1016/J.MICPATH.2020.104481

Kouchi, A. (2011). "Amorphous Carbon," *Encyclopedia of Astrobiology*, Springer, Berlin, Heidelberg, 41–42. DOI: 10.1007/978-3-642-11274-4_70

Li, J., Lyu, Y., Li, C., Zhang, F., Li, K., Li, X., Li, J., and Kim, K. H. (2023). "Development of strong, tough and flame-retardant phenolic resins by using Acacia mangium tannin-functionalized graphene nanoplatelets," *International Journal of Biological Macromolecules* 227, 1191–1202. DOI: 10.1016/J.IJBIOMAC.2022.11.305

Liu, X., Tan, W., Ye, Z., Zhang, Y., Ren, Y., and Liu, X. (2025). "Lignin-based flame retardants chelated with Fe3+: Facilitating the development of flame retardant, UV resistant and antibacterial properties polyvinyl alcohol composites," *International Journal of Biological Macromolecules* 286, 138182. DOI: 10.1016/J.IJBIOMAC.2024.138182

Ma, H., and Fang, Z. (2012). "Synthesis and carbonization chemistry of a phosphorous–nitrogen based intumescent flame retardant," *Thermochimica Acta* 543, 130–136. DOI: 10.1016/J.TCA.2012.05.021

Majka, T. M., Bartyzel, O., Raftopoulos, K. N., Pagacz, J., Leszczyńska, A., and Pielichowski, K. (2016). "Recycling of polypropylene/montmorillonite nanocomposites by pyrolysis," *Journal of Analytical and Applied Pyrolysis* 119, 1–7. DOI: 10.1016/J.JAAP.2016.04.005

Majka, T. M., Cokot, M., and Pielichowski, K. (2018). "Studies on the thermal properties and flammability of polyamide 6 nanocomposites surface-modified via layer-by-layer deposition of chitosan and montmorillonite," *Journal of Thermal Analysis and Calorimetry* 131(1), 405–416. DOI: 10.1007/S10973-017-6849-4/FIGURES/10

Majka, T. M., Bartyzel, O., Raftopoulos, K. N., Pagacz, J., and Pielichowski, K. (2019). "Examining the influence of re–used nanofiller—pyrolyzed montmorillonite, on the thermal properties of polypropylene–based engineering nanocomposites," *Materials 2019* 12(16), 2636. DOI: 10.3390/MA12162636

Majka, T. M., Witek, M., Radzik, P., Komisarz, K., Mitoraj, A., and Pielichowski, K. (2020). "Layer-by-layer deposition of copper and phosphorus compounds to develop flame-retardant polyamide 6/montmorillonite hybrid composites," *Applied Sciences 2020* 10(14), 5007. DOI: 10.3390/APP10145007

Majka, T. M. (2023a). "Flammability analysis of poly(ethylene terephthalate) and recycled PET with pyrolyzed filler," *Journal of Polymer Research* 30(9), 1–19. DOI: 10.1007/S10965-023-03737-Z/TABLES/7

Majka, T. M. (2023b). "The influence of amino chain length and calcium lignosulfonate modification on lignosulfonamides flammability and thermal stability," *Polimery* 68(10), 544–554. DOI: 10.14314/POLIMERY.2023.10.4

Majka, T. M., Piech, R., Piechaczek, M., and Ostrowski, K. A. (2024a). "The Influence of *Urtica dioica* and *Vitis vinifera* fibers on the thermal properties and flammability of polylactide composites," *Materials 2024* 17(6), 1256. DOI: 10.3390/MA17061256

Majka, T. M., Pimentel, A. C., Fernandes, S., de Almeida, H. V., Borges, J. P., and Martins, R. (2024b). "Experimental consideration of the effects of calcium lignosulfonate and tannic acid on the flammability and thermal properties of polylactide composites," *Thermochimica Acta* 737, 179769. DOI: 10.1016/J.TCA.2024.179769

Majka, T. M. (2024a). "Effect of LbL deposited chitosan-nanosilica bilayers on flammability and thermal properties of polylactide materials," *International Journal of Heat and Technology* 42(4), 1257–1269. DOI: 10.18280/IJHT.420416

Majka, T. M. (2024b). "Purification effect of pyrolyzed filler on the flammability of polylactide matrix," *Iranian Polymer Journal (English Edition)* 1–21. DOI: 10.1007/S13726-024-01396-5/FIGURES/5

Mansur, D., Sugiwati, S., Rizal, W. A., Suryani, R., and Maryana, R. (2023). "Pyrolysis of cajuput (*Melaleuca leucadendron*) twigs and rice (*Oryza sativa*) husks to produce liquid smoke-containing fine chemicals for antibacterial agent application," *Biomass Conversion and Biorefinery* 13(12), 10561–10574. DOI: 10.1007/S13399-021-01896-X/FIGURES/11

Meng, H., Wen, M., Shi, J., Liang, Y., and Jian, H. (2024). "Biomass flame retardants with application of cellulose, lignin, and hemicellulose from wood resources and their flame retardant technologies in related materials: A review," *Sustainable Chemistry and Pharmacy* 42, 101816. DOI: 10.1016/J.SCP.2024.101816

Montazeri, N., M Oliveira, A. C., Himelbloom, B. H., Beth Leigh, M., Crapo, C. A., Alexandra M Oliveira, C. C., and Seafood, K. (2013). "Chemical characterization of commercial liquid smoke products," *Food Science & Nutrition* 1(1), 102–115. DOI: 10.1002/FSN3.9

Morsy, N. F. S. (2015). "A short extraction time of high quality hydrodistilled cardamom (*Elettaria cardamomum* L. Maton) essential oil using ultrasound as a pretreatment," *Industrial Crops and Products*, Elsevier, 65, 287–292. DOI: 10.1016/J.INDCROP.2014.12.012

Moulai-Hacene, F., Boufadi, M. Y., Keddari, S., and Homrani, A. (2020). "Chemical composition and antimicrobial properties of *Elettaria cardamomum* extract," *Pharmacognosy Journal* 12(5), 1058–1063. DOI: 10.5530/pj.2020.12.149

Muchtaridi, Subarnas, A., Apriyantono, A., and Mustarichie, R. (2010). "Identification of compounds in the essential oil of nutmeg seeds (*Myristica fragrans* Houtt.) that inhibit locomotor activity in mice," *International Journal of Molecular Sciences* 11(11), 4771–4781. DOI: 10.3390/IJMS11114771

Ni, Y., Li, J., and Fan, L. (2020). "Production of nanocellulose with different length from ginkgo seed shells and applications for oil in water Pickering emulsions," *International Journal of Biological Macromolecules* 149, 617–626. DOI: 10.1016/J.IJBIOMAC.2020.01.263

Nie, S., Cui, S. W., and Xie, M. (2018). "Introduction," *Bioactive Polysaccharides* 1–50. DOI: 10.1016/B978-0-12-809418-1.00001-0

"Nutmeg, mace and cardamons (HS: 0908) Product Trade, Exporters and Importers | The Observatory of Economic Complexity." (n.d.). (https://oec.world/en/profile/hs/nutmeg-mace-and-cardamons), Accessed 28 Oct. 2024).

Renard, C. M. G. C. (2019). "Interactions Between Dietary Antioxidants and Plant Cell Walls," *Encyclopedia of Food Chemistry*, Academic Press, 633–643. DOI: 10.1016/B978-0-08-100596-5.21499-6

Saloko, S., Darmadji, P., Setiaji, B., and Pranoto, Y. (2014). "Antioxidative and antimicrobial activities of liquid smoke nanocapsules using chitosan and maltodextrin and its application on tuna fish preservation," *Food Bioscience* 7, 71–79. DOI: 10.1016/J.FBIO.2014.05.008

Salvia-Trujillo, L., Rojas-Graü, A., Soliva-Fortuny, R., and Martín-Belloso, O. (2015). "Physicochemical characterization and antimicrobial activity of food-grade emulsions and nanoemulsions incorporating essential oils," *Food Hydrocolloids* 43, 547–556. DOI: 10.1016/J.FOODHYD.2014.07.012

Schartel, B., Wilkie, C. A., and Camino, G. (2016a). "Recommendations on the scientific approach to polymer flame retardancy: Part 1—Scientific terms and methods," *Journal of Fire Sciences* 34(6), 447–467. DOI: 10.1177/0734904116675881

Schartel, B., Wilkie, C. A., and Camino, G. (2016b). "Recommendations on the scientific approach to polymer flame retardancy: Part 2—Concepts," *Journal of Fire Sciences* 35(1), 3–20. DOI: 10.1177/0734904116675370

Sen, S., Patil, S., and Argyropoulos, D. S. (2015). "Thermal properties of lignin in copolymers, blends, and composites: a review," *Green Chemistry* 17(11), 4862–4887. DOI: 10.1039/C5GC01066G

Singh, G., Kiran, S., Marimuthu, P., Isidorov, V., and Vinogorova, V. (2008). "Antioxidant and antimicrobial activities of essential oil and various oleoresins of *Elettaria cardamomum* (seeds and pods)," *Journal of the Science of Food and Agriculture* 88(2), 280–289. DOI: 10.1002/JSFA.3087

Singla, P., Mehta, R., Berek, D., and Upadhyay, S. N. (2012). "Microwave assisted synthesis of poly(lactic acid) and its characterization using size exclusion chromatography," *Journal of Macromolecular Science, Part A* 49(11), 963–970. DOI: 10.1080/10601325.2012.722858

Sun, P., Jia, P., Wang, W., Hong, N., Yu, F., Chen, D., Wang, B., Gui, Z., and Hu, Y. (2024). "Unlocking anti-aging potential: Flame retardants thrive without added antioxidants," *Composites Part B: Engineering* 279, 111450. DOI: 10.1016/J.COMPOSITESB.2024.111450

Tian, F., Wu, Y., Xu, H., Chen, H., Wang, B., Zhu, C., She, Y., Jin, Y., Liu, Y., Wang, S., and Xu, X. (2024). "Lignin-derived core-shell flame retardants for fire-safety rigid polyurethane (RPU) insulations," *Construction and Building Materials* 451, 138749. DOI: 10.1016/J.CONBUILDMAT.2024.138749

Truzzi, E., Marchetti, L., Bertelli, D., and Benvenuti, S. (2021). "Attenuated total reflectance–Fourier transform infrared (ATR–FTIR) spectroscopy coupled with chemometric analysis for detection and quantification of adulteration in lavender and *Citronella* essential oils," *Phytochemical Analysis* 32(6), 907–920. DOI: 10.1002/PCA.3034

Won, S., Jung, M., Bang, J., Cho, S. Y., Choi, I. G., and Kwak, H. W. (2024). "Lignin-based flame retardant via sequential purification-nanoparticle formation, and NP coupled chemical modification," *International Journal of Biological Macromolecules* 281, 136499. DOI: 10.1016/J.IJBIOMAC.2024.136499

Xia, Z., Kiratitanavit, W., Yu, S., Kumar, J., Mosurkal, R., and Nagarajan, R. (2018). "Fire retardants from renewable resources," *Advanced Green Composites* 275–320. DOI: 10.1002/9781119323327.CH11

Xin, X., Dell, K., Udugama, I. A., Young, B. R., and Baroutian, S. (2021). "Transforming biomass pyrolysis technologies to produce liquid smoke food flavouring," *Journal of Cleaner Production* 294, 125368. DOI: 10.1016/J.JCLEPRO.2020.125368

Xu, D. P., Li, Y., Meng, X., Zhou, T., Zhou, Y., Zheng, J., Zhang, J. J., and Li, H. Bin. (2017). "Natural antioxidants in foods and medicinal plants: Extraction, assessment and resources," *International Journal of Molecular Sciences* 18(1), 96. DOI: 10.3390/IJMS18010096

Yaman, S. (2004). "Pyrolysis of biomass to produce fuels and chemical feedstocks," *Energy Conversion and Management* 45(5), 651–671. DOI: 10.1016/S0196-8904(03)00177-8

Yang, T. T., Guan, J. P., Tang, R. C., and Chen, G. (2018). "Condensed tannin from *Dioscorea cirrhosa* tuber as an eco-friendly and durable flame retardant for silk textile," *Industrial Crops and Products* 115, 16–25. DOI: 10.1016/J.INDCROP.2018.02.018